NeuroImage 194 (2019) 128–135

Contents lists available at ScienceDirect

NeuroImage

journal homepage: www.elsevier.com/locate/neuroimage

Distinct neuronal entrainment to beat and meter: Revealed by simultaneous EEG-fMRI

Qiang Li [a], Guangyuan Liu [a,*], Dongtao Wei [b], Ying Liu [b], Guangjie Yuan [a], Gaoyuan Wang [c]

[a] College of Electronic and Information Engineering, Southwest University, No. 2, TianSheng Street, Beibei, Chongqing, 400715, China
[b] Department of Psychology, Southwest University, No. 2, TianSheng Street, Beibei, Chongqing, 400715, China
[c] College of Music, Southwest University, No. 2, TianSheng Street, Beibei, Chongqing, 400715, China

ARTICLE INFO

Keywords:
Single trial EEG-fMRI
Neuronal entrainment
Beat
Meter
The putamen

ABSTRACT

Rhythm perception refers to the mental interpretation of rhythm by a listener. Musical rhythm perception typically involves two steps: beat extraction and metrical structure assignment (meter perception). The entrainment theories propose that different neuronal oscillations entrain to different levels of metrical structure in the rhythm (e.g., beat and meter) and thereby form a representation of the rhythm in the mind. Thus, neuronal populations that entrain to beat and meter should theoretically be different. However, although entrainment theories have been supported by many studies, the neuronal populations that entrain to beat and meter remain largely unknown. In this study, we used a paradigm to induce neuronal entrainment to beat and meter and obtained images of the neuronal populations with an electroencephalogram functional magnetic resonance imaging (EEG-fMRI) fusion method. We observed that some neuronal populations, including the bilateral putamen, bilateral caudate, left thalamus, and supplementary motor area (SMA), entrain to both beat and meter. We also observed that the bilateral putamen entrains more to meter and the SMA entrains more to beat. Our results suggest that the bilateral putamen plays an important role in meter perception.

1. Introduction

The first step of rhythm perception is to extract the beat at a particular rate (the tempo) from the acoustic surface to serve as a basis for structuring and organizing incoming sonic events (Grahn, 2012; Levitin et al., 2017). After beat extraction, musical rhythm perception requires a second step, meter perception, which is also known as metrical structure assignment (Fitch, 2013; Grahn, 2012). Meter perception hierarchically organises beats into a metrical structure, which systematically attributes a particular perceptual prominence to each beat (Fitch, 2013; Grahn, 2012). This process allocates particular beats in the series as accented beats, even if they are physically identical to the other beats. In brief, a people may assign a meter of {**strong**, weak, **strong**, weak, …} to a series of identical beats (Nozaradan et al., 2011). The functional differences between beat extraction and meter perception hint different neural substrates underlying these two processes.

Models of musical rhythm perception range from rule-based models (Desain and Honing, 1999; Dillon, 1981; Povel and Essens, 1985) to entrainment models (Drake and Palmer, 1993; Eck, 2002; Large and Jones, 1999). Rule-based models assume that rhythm is perceived based on an internal clock and a pacemaker-accumulator mechanism. The assumed internal clock, which is also called pacemaker, ticks out regular intervals that correspond to beats in rhythms. The number of beats between accented beats enters an accumulator. The pacemaker-accumulator mechanism can therefore store the hierarchical structure of rhythm (Grahn, 2012). In contrast, the term entrainment refers to synchronising internal periodic processes to periodicities in external stimuli. The entrainment models of rhythm perception propose that beat extraction and meter perception emerge from the entrainment of neurons resonating to the beat and meter. These entrainment theories suggest that perception of rhythm is based on a differentiated neuronal entrainment mechanism, i.e., different neural populations in the brain entrain to different levels of metrical structure in the rhythm.

Nozaradan et al. (2011) have proposed an experimental design to assess whether scalp-recorded electroencephalogram (EEG) would resonate to beat and meter. In this experiment, participants were first asked to listen to isochronous beats and then imagine a binary or a ternary meter over the beats. They found that scalp-recorded EEG resonated to the beat and meter, thus forming auditory steady-state-evoked potentials (ASSEPs) to beat and meter. ASSEPs in scalp-recorded EEG stem from

* Corresponding author.
E-mail address: liugy@swu.edu.cn (G. Liu).

https://doi.org/10.1016/j.neuroimage.2019.03.039
Received 28 June 2018; Received in revised form 28 February 2019; Accepted 18 March 2019
Available online 23 March 2019

neural oscillations that resonate via entrainment to the frequency of external stimuli (Galambos et al., 1981; Large, 2008). Therefore, such findings provide evidence that there is neuronal entrainment to beat and meter. However, regrettably, due to the poor spatial resolution of EEG, the specific neuronal populations that entrained to beat and meter remain unknown.

Functional magnetic resonance imaging (fMRI) uses blood oxygenation level dependent (BOLD) response to measure neural activity with high spatial resolution. A fusion of fMRI and EEG may provide a solution for the limitation of low spatial resolution of EEG. Therefore, this could add to a more complete understanding of the neural basis of beat and meter perception. The biggest difficulty in EEG-fMRI fusion analysis is to find appropriate neural activity that can be captured by both EEG and fMRI. In the experiments of (Nozaradan et al., 2011), ASSEPs induced by beat and meter were generated by neural oscillations. The amplitudes of these neural oscillations inevitably fluctuate across blocks, which suggests there are fluctuations in oxygen consumption across blocks, and therefore, fluctuations in BOLD that can be captured by fMRI. Thus, neuronal entrainment to beat and meter can be captured by both EEG (ASSEPs) and fMRI (BOLD). This means that EEG-fMRI fusion analysis is suitable for locating the neuronal populations entrained to beat and meter.

In this study we use an EEG-fMRI method to locate neuronal populations entrained to beat and meter. Unlike traditional fMRI which generally assumes an identical response amplitude to identical stimuli, this EEG-fMRI method focuses on the fluctuations of ASSEPs across blocks. Given that the putamen has been observed to be involved in processes more complicated than beat perception (Grahn and Rowe, 2013, 2009; Lewis and Miall, 2003), we hypothesise that the putamen is the most likely candidate area that will entrain more to meter than to beat.

2. Material and methods

2.1. Participants

We recruited 31 healthy student participants (female, n = 16; age range: 19–23 years) from the College of Music at Southwest University. All participants were required to have over eight years' musical experience, either in singing training, instrument training, or dance training. All participants were Chinese and had no history of a hearing disorder. The hearing thresholds of all participants were tested and all were better than 25 dB, from 250 to 8000 Hz.

Ethics statement: All participants signed informed consent and the experimental paradigm was approved by the ethics committee of Southwest University (project number: H17022).

2.2. Experimental paradigm

The basic sound of the stimuli was a pure tone of 333 Hz. This pure tone was amplitude modulated by asymmetrical Hanning envelopes (with 5% rise time and 95% fall time) at 2.4 Hz, with amplitude modulation between 0 and 1. We chose the 2.4 Hz because this frequency and the imagined meter of 1.2 Hz (corresponding to 72 [1.2 Hz] and 144 [2.4 Hz] beats per minute [bpm]) are within the range of general musical tempo, which is 40–240 bpm (Moravcsik, 1987).

This sound signal was amplitude then modulated by an 11 Hz sinusoidal function with amplitude modulation between 0.3 and 1. The purpose of introducing the 11 Hz modulation was because 11 Hz is not an integral multiple of 1.2 and 2.4 Hz, introducing 11 Hz in these sounds would generate subtle irregularities in the envelope of the beats, resulting in a pseudo-periodic beat structure. This pseudo-periodic beat structure is closer to real musical beat structure than is a strict periodic beat structure (Nozaradan et al., 2011). Moreover, the two frequency amplitude modulations of 2.4 and 11 Hz can reduce the sideband frequency components of 2.4 Hz (i.e., 0.8 and 1.2 Hz) and thereby reduce the perception of binary meter in the beat perception condition (Nozaradan et al., 2011). The stimulus lasted 12.5 s with an average inter-stimulus interval of 5 s and a range of 4–6 s (Fig. 1). An example of the stimuli has been submitted as supplementary material.

In this study, active noise reduction headphones were used (OptoActive, OptoAcoustics, Mazor, Israel, http://www.optoacoustics.com/medical/optoactive/features). The headphones can actively reduce noise from MR echo-planar imaging (EPI) and has been widely used in acoustic fMRI studies (Özbay et al., 2018; Rosemann and Thiel, 2018; Yulia et al., 2017). The system requires 16 s to learn the noise of MR EPI and subsequently can actively reduce this noise. The intensity of the stimulus was calibrated by a Bruel & Kjaer 2236 sound meter (Bruel& Kjaer, Naerum, Denmark) and adjusted to 75 dB.

Participants completed two tasks. First, in the beat perception condition, participants were told to stay awake and listen to the sounds with no specific task performed. This represented the control condition. Second, participants completed the binary meter imagery condition after the beat perception condition. Participants went back to the monitor room accompanied by an experimenter and were instructed to imagine a binary metric structure (1.2 Hz) over the beat. Participants listened to the stimulus and imagined the following binary metric structure over the beat: {**strong**, weak, **strong**, weak}. Under the guidance of the experimenter, they were asked to tap along with the imagined {**strong**, weak, **strong**, weak} metric structure. Once they were able to tap along with the binary metric structure alone, they were told to just imagine it during the presentation of the stimulus, but not to tap. Participants were given the opportunity to practise, and training ended when the participant reported that he/she could imagine the metric structure over the beats without tapping. Subsequently, participants were told to imagine the same binary meter over the beats during the next experimental session but not to tap. Imagery guidance was given after the beat perception condition to exclude the influence of the imagery guidance on beat perception. For both tasks, the stimulus was played thirty times.

This experimental paradigm is very similar to that of Nozaradan et al. (2011), but two main changes were made to adapt to the MRI environment. First, we did not conduct a task in which participants imagined a ternary meter, because beat listening and binary meter imagery tasks are sufficient to meet our aims. Second, we increased the number of blocks

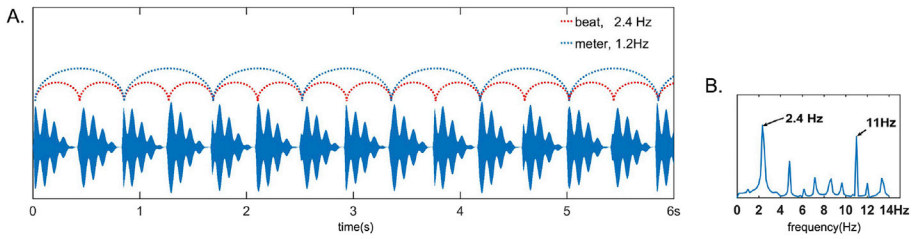

Fig. 1. A. A 6 s excerpt of the sound wave. The pseudo-periodic beat structure is closer to real musical beat and meter structure, and it can reduce sideband interference. Beat perception is shown with a red line and binary meter imagination is show in blue. **B.** Frequency spectrum of the envelope of the sound wave.

from 10 to 30, to make the experiment suitable for fMRI analysis. We also shortened the blocks from 33 s to 12.5 s to shorten the length of the meter imagery task. In the pilot experiment, participants reported that they failed to imagine a meter over the beat at the end of the experiment because their attention wandered when the experiment was longer than 15 min. Therefore, by shortening a block to 12.5 s we shortened the task to about 10 min. During debriefing, 28 participants reported that they were able to continue imagining the meter for the whole metre imagery task and only three participants reported that they occasionally failed to imagine the meter during the last two minutes of the task.

2.3. Simultaneous acquisition of EEG and fMRI

In this study, EEG and fMRI were simultaneously recorded. EEG was recorded simultaneously with fMRI with an MRI-compatible EEG recording system (BrainAmp MR plus, Brain Products, Munich, Germany). EEG was recorded across 32 channels, with an electrode recording electrocardiogram (ECG). The sample rate was 5000 Hz, electrodes were placed according to the International 10/20 system, and electrode impedance was kept below 10 kΩ.

FMRI data was recorded with a 3T Siemens scanner. We used a continuous scanning sequence with the following parameters: repetition time (TR), 2s; echo time (TE), 26 ms; voxel size, 3*3*3 mm; flip angle, 90°; 32 slices. For each run, there were 310 scans and the first 10 scans were used to train the earphone system without playing stimuli. After the two tasks were finished, high resolution T1 images were acquired with the following parameters: TR, 1900 ms; TE, 2.52 ms; voxel size, 1*1*1 mm, and 176 slices.

Data and code availability statement: Data not available/The data that has been used is confidential.

Due to the potential value that has not been fully explored by the current manuscript, survey respondents were assured raw data and code would remain confidential and would not be shared.

2.4. EEG analysis

2.4.1. EEG preprocessing

EEG preprocessing was conducted in Matlab (2015b) (Mathworks, Natick, MA) and Analyzer 2.1 (Brain Products). Noise reduction was conducted to eliminate fMRI gradient artifacts, ballistocardiogram (BCG) artifacts, and ocular artifacts. First, we used Analyzer 2.1 to eliminate fMRI gradient artifacts. EEG were re-referenced to averaged TP9/TP10 and a local average artifact procedure was used to eliminate fMRI gradient artifacts (Allen et al., 2000). Cut off frequency was set as 70 Hz. Subsequently, EEG were downsampled to 500 Hz. Second, we used EEGLAB 13 and the toolbox FMRIB 2.0 (Niazy et al., 2005) to eliminate BCG artifacts. The latter toolbox removes BCG artifacts with optimal basis sets. Third, we eliminated ocular artifacts with the function 'Ocular remove using ICA' of Analyzer 2.1. Finally, EEG data was exported to EEGLAB 13 and high-pass filtered (>0.1 Hz) to remove very slow shifts.

2.4.2. EEG analysis

EEG epochs were extracted from −100 ms to 12.5 s relative to the onset of the auditory stimuli and the baseline was set as −10–0 ms. ASSEPs were segmented from 2.5 s to 12.5 s relative to the onset of the stimuli. Data from −0.1–2.5 s was discarded because event-related potentials (ERPs) to the first tone were typical auditory ERPs with P1, N1, and P2 components, and several repetitions of beats are required to reach a steady state evoked response (Repp, 2005). The frequency spectra of ASSEPs to beat and metre were obtained using Fourier transform (Frigo and Johnson, 2002; Nozaradan et al., 2011). Topographical maps of ASSEPs to beat and metre were drawn at the target frequencies.

One-sample t tests were used to examine whether perception of beat and metre generated a significant steady state response. Amplitudes at target frequencies (f) were tested against amplitudes of frequencies of (f±0.5 Hz). If there is a steady state response, amplitudes of ASSEPs to beat and metre should be significantly different to amplitudes not within the target frequencies.

2.5. fMRI preprocessing

A standard preprocessing processing stream was conducted to fMRI data under the guidance of the SPM12 Manual (http://www.fil.ion.ucl.ac.uk/spm/). The steps included head motion correction, slice timing correction, coregistration to anatomic structure, spatial normalization and spatial smoothing.

2.6. fMRI and EEG-fMRI fusion analysis

fMRI and EEG-fMRI fusion data were analysed in Matlab (2015b), and SPM12 and EEGLAB 13 were also used. Single trial ERPs were collected from a pooled electrode (Cz/FC1/FC2) because paradigm-induced ASSEPs are maximally expressed in frontocentral and temporal regions (Nozaradan et al., 2011). Indeed, our results were consistent with this, with ASSEPs maximally expressed at Cz, FC1, and FC2 (Fig. 2B).

For each condition (beat and meter), two regressors were designed. One regressor was designed for conventional fMRI analysis, formed by convolving the onset times of blocks and a canonical haemodynamic response function, with the 'duration of stimuli' set as 12.5 s. This regressor encoded a generic obligatory response of constant amplitude, without considering fluctuations of response amplitudes. Another regressor was designed for the EEG-fMRI analysis, which was parametrically modulated by the amplitude fluctuations of ASSEPs across blocks. This regressor represented fluctuations in amplitudes of neuronal entrainment to beat and meter across blocks. The amplitudes of ASSEPs across blocks in the two conditions were extracted to form ASSEPs amplitude vectors. Vectors for ASSEPs across blocks were used to amplitude modulate the onset times of blocks and formed the AM vectors. Amplitude modulation (AM) vectors were orthogonalised with the onset times of blocks to ensure they were specific to fluctuations in ASSEPs (Eichele et al., 2005; Mulert et al., 2008). These orthogonalised AM vectors were convolved with a canonical haemodynamic response function to construct regressors for EEG-fMRI analysis, with the 'duration of stimuli' set as 12.5 s (Fig. 3).

Therefore, there were two conventional regressors (corresponding to beat and meter) and two corresponding ASSEPs AM regressors. These four regressors, together with six head motion regressors, were entered into a single-subject fixed effects analysis using general linear model (GLM) analysis. In the group-level analysis, random effects analysis was executed across the 31 participants with significance set as $p < .05$ (cluster–extent family-wise error (FWE) corrected; voxel-height threshold, $p < .005$; extent, 10 voxels).

3. Results

3.1. EEG results

Fig. 2 presents the group average EEG results and Fig. 2A presents ERPs for the first 700 ms in the two conditions. These ERPs are typical auditory evoked potentials, with P1, N1, and P2 components. Fig. 2C presents transient ERPs to beat and meter from the pooled electrodes Cz/FC1/FC2. These ERPs can be divided into two parts: i) −100–700 ms, typical auditory evoked potentials; and ii) 2.5–12.5 s, ASSEPs. Frequency spectra for ASSEPs to beat and meter and topographical maps of the two conditions are presented in Fig. 2B. ASSEPs to beat and meter were segmented from 2.5 s to 12.5 s. The amplitudes of ASSEPs to beat and meter from the Cz/FC1/FC2 electrodes were 0.34 μV and 0.33 μV, respectively. Moreover, there were ASSEPs to 2.4 Hz in the meter condition, with an amplitude of 0.24 μV. These results are shown in Table 1.

There was a significant difference between ASSEPs to beat in the two conditions ($t = 12.9$, $p < .001$). Furthermore, there was a significant increase in the amplitudes of ASSEPs in the beat condition ($t = 24.5$,

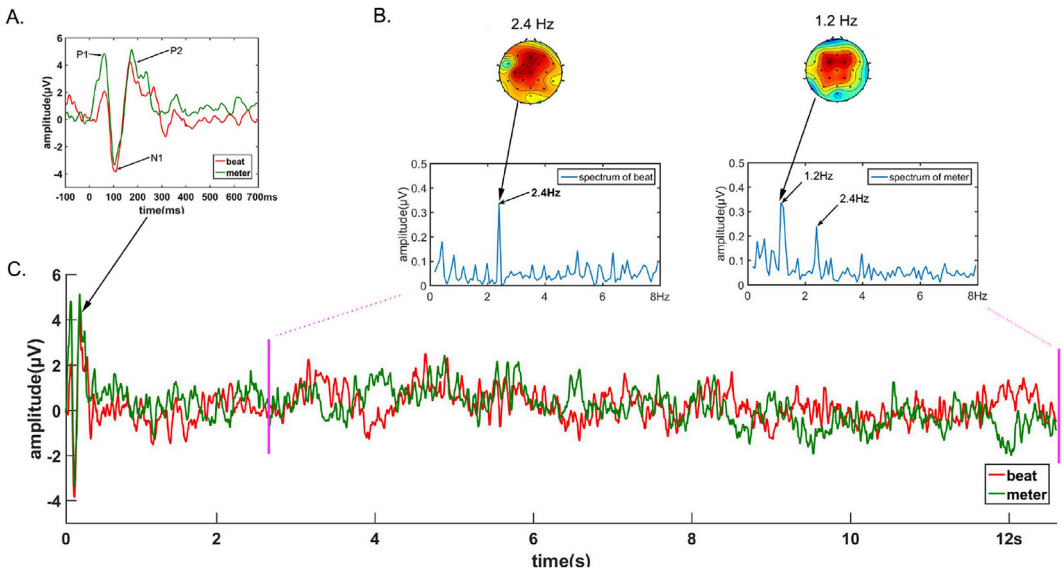

Fig. 2. Group average event-related potentials (ERPs). **A.** Typical auditory evoked potentials with P1, N1, and P2 components were observed from −100 ms to 700 ms for both conditions. **B.** Topographical maps of auditory steady-state evoked potentials (ASSEPs) and spectra of ASSEPs to beat and meter. **C.** Transient ERPs to beat and meter.

$p < .001$, 2.4 Hz vs. 1.9 Hz; $t = 28.6$, $p < .001$, 2.4 Hz vs. 2.9 Hz), and in the meter condition ($t = 12.4$, $p < .001$, 1.2 Hz vs. 0.7 Hz; $t = 26.3$, $p < .001$, 1.2 Hz vs. 1.7 Hz; $t = 12.1$, $p < .001$, 2.4 Hz vs. 1.9 Hz; $t = 16.3$, $p < .001$, 2.4 Hz vs. 2.9 Hz). Scalp maps showed that ASSEPs were primarily distributed across the frontal central areas. These results are shown in Table 2.

3.2. fMRI results

For conventional fMRI analysis, a conjunction analysis of beat and metre (beat + meter) showed activation in the bilateral primary auditory cortex (PAC), bilateral precentral gyrus (PCG), and SMA. Random effects analysis of beat vs. meter showed weak activation in the bilateral PCG and SMA. There were no significant regions of activation for the meter vs. beat condition. Results of conventional fMRI analysis are presented in Fig. 4A and Table 3.

3.3. EEG-fMRI results

For EEG-fMRI fusion analysis common activations for beat and meter (beat + meter) were observed in the bilateral putamen, bilateral caudate, left thalamus, and SMA. Analysis of meter vs. beat indicated significant activation in the bilateral putamen, while beat vs. meter indicated activation in the SMA. Results of EEG-fMRI analysis are presented in Fig. 4B and Table 4.

4. Discussion

In this study we used an EEG-fMRI fusion method to locate neuronal populations that entrain to beat and meter. According to the entrainment theory, neuronal populations that entrain to beat and meter should be different. Our results support this hypothesis, as we found that while there are common neural substrates underlying perception of beat and meter, the bilateral putamen entrains more to meter while the SMA entrains more to beat.

Our conventional transient ERP results were consistent with the previous findings of Nozaradan et al. (2012, 2011). Brain responses to the first beat of the stimulus were represented by typical auditory evoked potentials, with P1, N1, and P2 components. After several repeats of the beats, ASSEPs to beat or meter emerged. For the beat condition, ASSEPs to beat were observed with a peak of 2.4 Hz in the frequency spectrum. Two ASSEPs were observed in the meter condition, one to meter at a frequency of 1.2 Hz and to beat at a frequency of 2.4 Hz. Our result showing ASSEPs in response to metre is consistent with findings that neuronal entrainment to beat and meter can be directly captured by scalp recorded EEG (Nozaradan et al., 2011).

Moreover, in line with previous findings, our conventional fMRI results from a conjunction analysis of beat and meter indicated activation in the bilateral PAC, bilateral PCG, and SMA (Chen et al., 2008; Costa-Faidella et al., 2017; Grahn and Rowe, 2013, 2009; Luke et al., 2017; Morillon and Baillet, 2017; Teki et al., 2011; Zatorre et al., 2007). Importantly, in the contrast of beat vs. meter, the SMA was also observed to show activation. This result suggests that imagery of meter leads to a weakened response in the SMA in beat perception and that the SMA is not the core area of metrical structure assignment.

Many efforts have been made to illustrate the neural basis of rhythm perception (Chen et al., 2008; Ehrsson et al., 2009; Fitch, 2013; Grahn and Brett, 2007; Lewis et al., 2004; Vaquero et al., 2018), with results indicating a role of the SMA, premotor cortex, basal ganglia, and cerebellum in musical rhythm perception. Indeed, these regions form the motor cortico-basal ganglia-thalamo-cortical (mCBGT) circuit, which is considered the neural basis of rhythm perception (Merchant et al., 2015). Our EEG-fMRI results showed common neuronal populations that entrain to beat and meter, including the bilateral putamen, bilateral caudate, left thalamus, and SMA. Moreover, our fusion results support the mCBGT theory and extend entrainment model by providing evidence that the neuronal populations entrained to different levels of metrical structure are not completely different but partially overlap.

Furthermore, our EEG-fMRI results indicate distinct neuronal entrainment to beat and meter, with the bilateral putamen entraining more to meter and the SMA entraining more to beat. The role of the putamen in meter perception is worth exploring further. Some models of rhythm perception (Desain and Honing, 1999; Dillon, 1981; Povel and Essens, 1985) and timing (Church and Broadbent, 1990; Gibbon, 1977) share a similar hypothesis that the internal representation of rhythm or timing comprises three components: an internal clock, a pacemaker-accumulator with memory, and a matching mechanism. These models can be simplified as an internal clock that serves as a neural pacemaker, which continually emits pulses. The pacemaker-accumulator accumulate and store the number of pulses between accented beats and thus form a mental interpretation of rhythm. According to our EEG-fMRI results, it seems that during rhythm perception, the SMA, bilateral

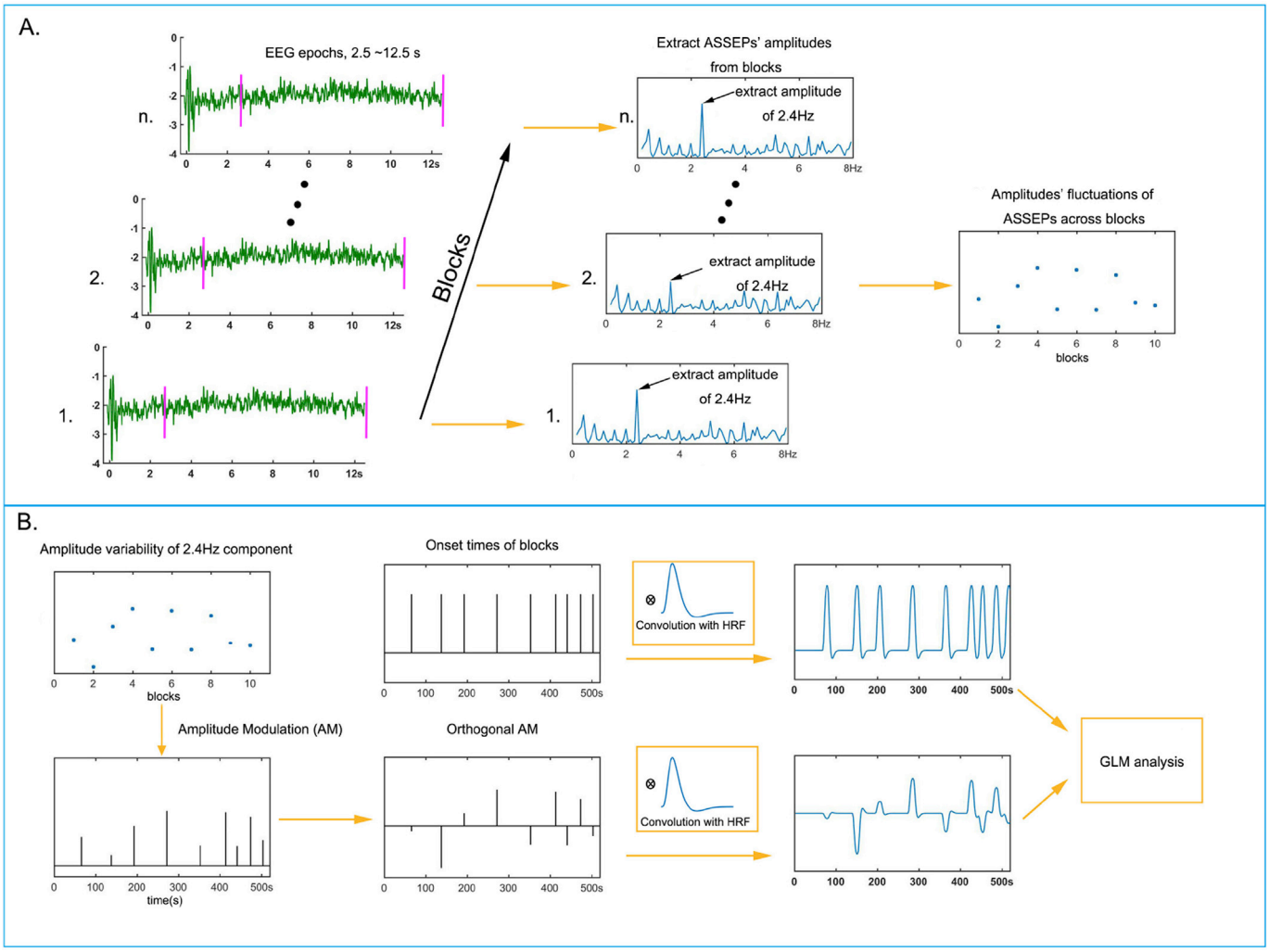

Fig. 3. Flowchart of electroencephalogram-functional magnetic resonance imaging (EEG-fMRI) analysis. **A.** Extracting amplitudes of auditory steady-state evoked potentials (ASSEPs) across blocks. **B.** General linear model (GLM) analysis. Amplitudes of ASSEPs to beat or meter were used to modulate the amplitudes of conventional regressors. The amplitude-modulated regressors were convolved with a haemodynamic response function and entered into GLM analysis together with the conventional regressors.

Table 1
EEG results.

Conditions	ASSEPs to beat	ASSEPs to meter	P1	N1	P2
beat	0.34 μV	–	2.07 μV	−3.81 μV	4.18 μV
meter	0.24 μV	0.33 μV	4.86 μV	−3.33 μV	5.13 μV

Table 2
Significance of increase in amplitude of ASSEPs.

Conditions	2.4 Hz vs. 1.9 Hz	2.4 Hz vs. 2.9 Hz	1.2 Hz vs. 0.7 Hz	1.2 Hz vs. 1.7 Hz
beat	$t = 24.5$, $p < .001$	$t = 28.6$, $p < .001$	–	–
meter	$t = 12.1$, $p < .001$	$t = 16.3$, $p < .001$	$t = 12.4$, $p < .001$	$t = 26.3$, $p < .001$

putamen, bilateral caudate, and left thalamus serve as an internal clock network and the bilateral putamen plays the role of the pacemaker-accumulator. Oscillations of the internal clock network resonate at the frequency of the beat and form an internal clock. The bilateral putamen accumulates and stores the number of beats between accented beats. After several repetitions of the rhythm, the metrical structure stored in the putamen becomes more robust. When the number of incoming pulses matches the stored number, the putamen triggers the internal clock network to activate, thereby generating oscillations resonating at the frequency of meter.

This hypothesis is consistent with the preference for an integer ratio relationship during perception of rhythm. Several rhythm perception studies have reported that rhythms encoded in integer ratio relationships to a beat are reproduced more accurately than rhythms that are not (Essens and Povel, 1985; Patel et al., 2005). Some participants even reproduce integer ratio rhythms by regularizing perceived non-integer ratio rhythms (Collier and Wright, 1995; Essens, 1986). Our internal clock-accumulator hypothesis can explain these phenomena well because the internal clock resonates at the frequency of the beat, and the putamen can only match an integer ratio interval of the beat.

Our results also suggest that during the meter imagery task, there was weakening of ASSEPs to the beat, fMRI activation in the SMA and precentral area, and neuronal entrainment in the SMA. In contrast to the high-level role of the putamen in perceiving rhythm, the SMA has more often been found to be activated when automatically perceiving a beat (Ivry and Spencer, 2004; Lewis and Miall, 2003). These results suggest a competitive relationship between cognitively-controlled meter perception and automatic perception of beat.

It worth discussing why traditional fMRI is not suitable to identify the

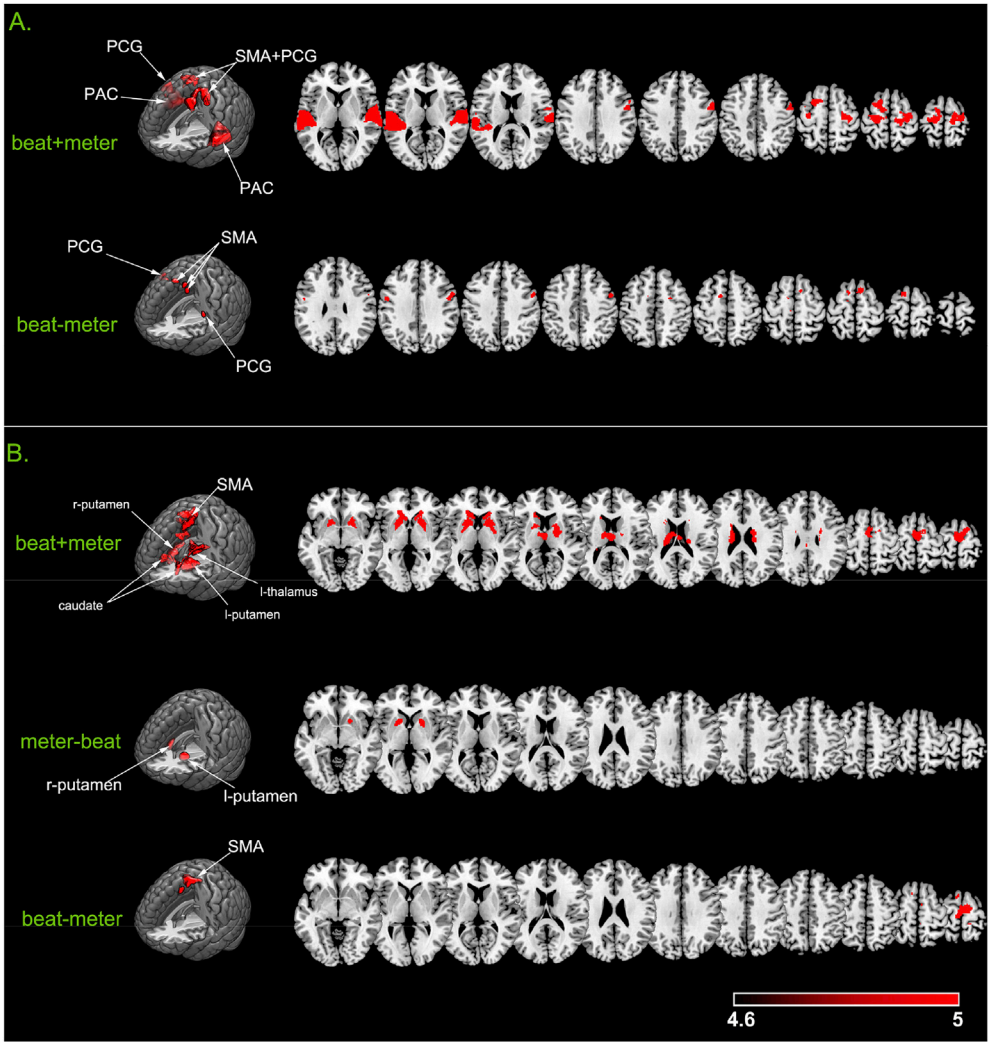

Fig. 4. Functional magnetic resonance imaging (fMRI) and electroencephalogram-fMRI (EEG-fMRI) results. **A.** FMRI results. The first row shows results for beat + meter, with activation in the primary auditory cortex (PAC), precentral gyrus (PCG), and supplementary motor area (SMA). The second row shows results for beat-meter, with activation in the SMA and bilateral PCG. **B.** EEG-fMRI results. For beat + meter, there was activation in the bilateral putamen, bilateral caudate, left thalamus, and SMA. For meter-beat, there was activation of the bilateral putamen and for beat-meter, the SMA was activated. All results are family-wise error corrected, $p < .05$ (voxel-height threshold, $p < .005$; extent, 10 voxels).

Table 3
fMRI results.

condition	Region	Num of voxels	T	+/−	MNI coordinates		
					x	y	z
beat + meter	Temporal_Sup_R	1176	9.42	pos	68	−20	6
	Temporal_Sup_L	1396	8.84	pos	−60	−16	6
	Precentral_L	681	6.69	pos	−22	−20	66
	Precentral_R	583	6.73	pos	34	−20	58
	Precentral_R	236	6.44	pos	54	0	42
	Precentral_R	29	6.14	pos	64	−4	14
beat-meter	Precentral_R	117	5.51	pos	54	6	38
	Precentral_L	34	6.04	pos	−50	−2	34
	Supp_Motor_Area_L	35	5.92	pos	−12	2	54
	Supp_Motor_Area_R	70	6.44	pos	10	12	66
	Supp_Motor_Area_L	47	7.01	pos	−12	8	68

neural substrate underlying perception of beat and meter, but has only been able to indicate a role for the PAC and SMA. Traditional event-related fMRI generally assumes the brain responds to identical stimuli with an identical amplitude. However, brain states inevitably ebb and flow over time and, thus, the brain may respond to identical stimuli with different amplitudes. We refer to this phenomenon as fluctuations across trials/blocks. If we can trace these fluctuations and use them to parameter modulate the regressor representing brain activity, we can obtain a regressor that more accurately reflects actual brain activation and thus make more precise localisation. The methodology in this paper follows this argument. Although neuronal populations resonate with beat and/or meter all the time, the amplitude of resonance inevitably fluctuates across blocks. We extracted these fluctuations from scalp-recorded EEG and used them to parameter modulate the regressors. These regressors better fitted actual activity in neuronal populations entrained to beat and meter. Therefore, they provide greater insight into the neural substrate underlying perception of beat and meter.

One limitation of this paper is that in the meter imagery condition, brain activity may be confounded by remembering or imagining tapping the meter. Although the imagined {**strong**, weak, **strong**, weak} meter

Table 4
EEG-fMRI results.

condition	Region	Num of voxels	T	+/−	MNI coordinates		
					x	y	z
beat + meter	Putamen_R	637	5.64	pos	20	16	2
	Putamen_L	413	5.12	pos	−18	16	2
	Supp_Motor_Area_R	760	6.12	pos	4	−14	70
	Caudate_L	241	5.49	pos	−14	24	4
	Caudate_R	173	5.50	pos	20	−6	26
	Thalamus_L	590	6.13	pos	−12	−8	14
meter-beat	Putamen_R	149	5.10	pos	20	12	2
	Putamen_L	138	5.21	pos	−18	18	2
beat-meter	Supp_Motor_Area_R	351	5.67	pos	6	−12	70
	Supp_Motor_Area_L	45	4.92	pos	−8	10	66

was emphasised, tapping during training may more or less influence the following task. Although there might be some latent motor activity in the metre imagery task, we believe its influence would be relatively slight.

5. Conclusion

In this study, we used an EEG-fMRI fusion method to locate neuronal populations that entrain to beat and meter. We observed that some neuronal populations including the SMA, bilateral putamen, bilateral caudate, and left thalamus entrain to both beat and meter. We also observed that the bilateral putamen entrains more to meter, while the SMA entrains more to beat.

Acknowledgements

This research was supported by the National Natural Science Foundation of China (61472330, 61872301 and 61502398).

Appendix A. Supplementary data

Supplementary data to this article can be found online at https://doi.org/10.1016/j.neuroimage.2019.03.039.

References

Allen, P.J., Josephs, O., Turner, R., 2000. A method for removing imaging artifact from continuous EEG recorded during functional MRI. Neuroimage 12, 230–239. https://doi.org/https://doi.org/10.1006/nimg.2000.0599.

Chen, J.L., Penhune, V.B., Zatorre, R.J., 2008. Listening to musical rhythms recruits motor regions of the brain. Cerebr. Cortex 18, 2844–2854. https://doi.org/10.1093/cercor/bhn042.

Church, R.M., Broadbent, H.A., 1990. Alternative representations of time, number, and rate. Cognition 37, 55–81.

Collier, G.L., Wright, C.E., 1995. Temporal rescaling of sample and complex rations in rhythmic tapping. J. Exp. Psychol. Hum. Percept. Perform. 21, 602.

Costa-Faidella, J., Sussman, E.S., Escera, C., 2017. Selective entrainment of brain oscillations drives auditory perceptual organization. Neuroimage 159, 195–206. https://doi.org/10.1016/j.neuroimage.2017.07.056.

Desain, P., Honing, H., 1999. Computational models of beat induction: the rule-based approach. J. New Music Res. 28, 29–42.

Dillon, H., 1981. The perception of musical instruments. Perception 11, 115–128.

Drake, C., Palmer, C., 1993. Accent structures in music performance. Music Percept. Interdisciplinaria J. 10, 343–378.

Eck, D., 2002. Finding downbeats with a relaxation oscillator. Psychol. Res. 66, 18–25.

Ehrsson, H.H., Hashimoto, T., Bengtsson, S.L., Ulle, F., Kito, T., Naito, E., Forssberg, H., Sadato, N., 2009. Listening to Rhythms Activates Motor and Premotor Cortices, vol. 45, pp. 62–71. https://doi.org/10.1016/j.cortex.2008.07.002.

Eichele, T., Specht, K., Moosmann, M., Jongsma, M.L.A., Quiroga, R.Q., Nordby, H., Hugdahl, K., 2005. Assessing the spatiotemporal evolution of neuronal activation with single-trial event-related potentials and functional MRI. Proc. Natl. Acad. Sci. U. S. A 102, 17798–17803. https://doi.org/10.1073/pnas.0505508102.

Essens, P.J., 1986. Hierarchical organization of temporal patterns. Attention, Perception, Psychophysiology 40, 69–73.

Essens, P.J., Povel, D.-J., 1985. Metrical and nonmetrical representations of temporal patterns. Percept. Psychophysiology 37, 1–7.

Fitch, W.T., 2013. Rhythmic cognition in humans and animals: distinguishing meter and pulse perception. Front. Syst. Neurosci. 7, 1–16. https://doi.org/10.3389/fnsys.2013.00068.

Frigo, M., Johnson, S.G., 2002. FFTW: an Adaptive Software Architecture for the FFT.

Galambos, R., Makeig, S., Talmachoff, P.J., 1981. A 40-Hz auditory potential recorded from the human scalp. Proc. Natl. Acad. Sci. Unit. States Am. 78, 2643 LP-2647. https://doi.org/10.1073/pnas.78.4.2643.

Gibbon, J., 1977. Scalar expectancy theory and Weber's law in animal timing. Psychol. Rev. 84, 279–325.

Grahn, J.A., 2012. Neural mechanisms of rhythm Perception . Current Findings and Future Perspectives 4, 585–606. https://doi.org/10.1111/j.1756-8765.2012.01213.x.

Grahn, J.A., Brett, M., 2007. Rhythm and Beat Perception in Motor Areas of the Brain, pp. 893–906.

Grahn, J.A., Rowe, J.B., 2013. Finding and feeling the musical beat: striatal dissociations between detection and prediction of regularity. Cerebr. Cortex 23, 913–921. https://doi.org/10.1093/cercor/bhs083.

Grahn, J.A., Rowe, J.B., 2009. Feeling the beat: premotor and striatal interactions in musicians and nonmusicians during beat perception. J. Neurosci. 29, 7540–7548. https://doi.org/10.1523/JNEUROSCI.2018-08.2009.

Ivry, R.B., Spencer, R.M.C., 2004. The neural representation of time. Curr. Opin. Neurobiol. 14, 225–232.

Large, E.W., 2008. Resonating to musical rhythm: theory and experiment. In: Grondin, S. (Ed.), The psychology of time. Emerald, West Yorkshire, UK, pp. 189–232.

Large, E.W., Jones, M.R., 1999. The dynamics of attending: how people track time-varying events. Psychol. Rev. 106, 119.

Levitin, D.J., Grahn, J.A., London, J., 2017. The Psychology of Music : Rhythm and Movement, pp. 1–25.

Lewis, P.A., Miall, R.C., 2003. Distinct systems for automatic and cognitively controlled time measurement: evidence from neuroimaging. Curr. Opin. Neurobiol. 13, 250–255.

Lewis, P.A., Wing, A.M., Pope, P.A., Praamstra, P., Miall, R.C., 2004. Brain activity correlates differentially with increasing temporal complexity of rhythms during initialisation, synchronisation, and continuation phases of paced finger tapping. Neuropsychologia 42, 1301–1312. https://doi.org/https://doi.org/10.1016/j.neuropsychologia.2004.03.001.

Luke, R., De Vos, A., Wouters, J., 2017. Source analysis of auditory steady state responses in acoustic and electric hearing. Neuroimage 147, 568–576.

Merchant, H., Grahn, J., Trainor, L., Rohrmeier, M., Fitch, W.T., 2015. Finding the beat: a neural perspective across humans and non-human primates. Philos. Trans. R. Soc. B Biol. Sci. 370. https://doi.org/10.1098/rstb.2014.0093.

Moravcsik, M.J., 1987. Musical Sound : an Introduction to the Physics of Music. Kluwer Academic/Plenum Publishers.

Morillon, B., Baillet, S., 2017. Motor origin of temporal predictions in auditory attention. Proc. Natl. Acad. Sci. Unit. States Am. 114, E8913–E8921. https://doi.org/10.1073/pnas.1705373114.

Mulert, C., Seifert, C., Leicht, G., Kirsch, V., Ertl, M., Karch, S., Moosmann, M., Lutz, J., Möller, H.-J., Hegerl, U., Pogarell, O., Jäger, L., 2008. Single-trial coupling of EEG and fMRI reveals the involvement of early anterior cingulate cortex activation in effortful decision making. Neuroimage 42, 158–168. https://doi.org/https://doi.org/10.1016/j.neuroimage.2008.04.236.

Niazy, R.K., Beckmann, C.F., Iannetti, G.D., Brady, J.M., Smith, S.M., 2005. Removal of FMRI environment artifacts from EEG data using optimal basis sets. Neuroimage 28, 720–737. https://doi.org/https://doi.org/10.1016/j.neuroimage.2005.06.067.

Nozaradan, S., Peretz, I., Missal, M., Mouraux, A., 2011. Tagging the neuronal entrainment to beat and meter. J. Neurosci. 31, 10234–10240. https://doi.org/10.1523/JNEUROSCI.0411-11.2011.

Nozaradan, S., Peretz, I., Mouraux, A., 2012. Selective neuronal entrainment to the beat and meter embedded in a musical rhythm. J. Neurosci. 32, 17572–17581. https://doi.org/10.1523/JNEUROSCI.3203-12.2012.

Özbay, P.S., Chang, C., Picchioni, D., Mandelkow, H., Thomas, M., Chappel-farley, M.G., Gelderen, P. Van, Zwart, J.A. De, Duyn, H., 2018. Contribution of Systemic Vascular Effects to (This). https://doi.org/10.1016/j.neuroimage.2018.04.045.

Patel, A.D., Iversen, J.R., Chen, Y., Repp, B.H., 2005. The influence of metricality and modality on synchronization with a beat. Exp. Brain Res. 163, 226–238.

Povel, D.-J., Essens, P., 1985. Perception of temporal patterns. Music Percept. Interdisciplinaria J. 2, 411–440.

Repp, B.H., 2005. Sensorimotor Synchronisation; a review of the tapping litterature. Pschonom Bulleti & Rview 12, 969–992.

Rosemann, S., Thiel, C.M., 2018. SC (This). https://doi.org/10.1016/j.neuroimage.2018.04.023.

Teki, S., Grube, M., Kumar, S., Griffiths, T.D., 2011. Distinct neural substrates of duration-based and beat-based auditory timing. J. Neurosci. 31, 3805–3812. https://doi.org/10.1523/JNEUROSCI.5561-10.2011.

Vaquero, L., Ramos-escobar, N., Rodríguez-fornells, A., 2018. NeuroImage White-matter Structural Connectivity Predicts Short-Term Melody and Rhythm Learning in Non-musicians, vol. 181, pp. 252–262.

Yulia, L., Maya, B., Shimrit, S., Galit, S., Tamir, E., Waheed, M., Alon, S., Talma, H., Ilana, K., Maya, B., Shimrit, S., Galit, Y., Tamir, E., Waheed, M., Alon, S., Talma, H., Ilana, K., 2017. PT SC.

Zatorre, R.J., Chen, J.L., Penhune, V.B., 2007. When the brain plays music: auditory-motor interactions in music perception and production. Nat. Rev. Neurosci. 8, 547–558. https://doi.org/10.1038/nrn2152.